ARCHIVES OF CIVIL AND MECHANICAL ENGINEERING 15 (2015) 335–346

Available online at www.sciencedirect.com

ScienceDirect

journal homepage: http://www.elsevier.com/locate/acme

Original Research Article

Experimental studies on ultrasonically assisted friction stir spot welding of AA6061

Y. Rostamiyan [a], A. Seidanloo [a], H. Sohrabpoor [b], R. Teimouri [c,*]

[a] Department of Mechanical Engineering, Sari Branch, Islamic Azad University, Sari, Iran
[b] Department of Mechanical Engineering, Dezful Branch, Islamic Azad University, Dezful, Iran
[c] Department of Mechanical Engineering, Babol University of Technology, Babol, Iran

ARTICLE INFO

Article history:
Received 28 April 2014
Accepted 24 June 2014
Available online 25 July 2014

Keywords:
US vibration
Friction stir spot welding
Experimental study

ABSTRACT

The present study introduces a new combination of two separate welding processes, i.e. friction stir spot welding (FSSW) and ultrasonic welding (USW). Here, in order to improve the weld quality, the friction stir spot welding is assisted by ultrasonic vibration of tool. To systematically analyze effect of process factors such as US vibration, tool rotary speed, tool plunge depth and dwell time on lap shear force and hardness, a L_{18} orthogonal array from Taguchi design of experiments is developed. Effects of process factors on responses were studied along with their percentage of contribution which was determined through analysis of variances. Results indicated that US vibration is a significant factor having positive influence on lap shear force and hardness. Next to the vibration, tool rotary speed, dwell time and plunge depth are also the important factors which affects mechanical properties significantly. Optimization of process factors by grey relational analysis showed that applying US vibration and selections of 1200 RPM tool rotary speed, 6 mm plunge depth and 6 s dwell time causes the highest value of grey relational grade and guarantee maximum lap shear force as well as maximum hardness.

1. Introduction

To meet the challenges for future automotive regarding emissions, safety, and sustainability, aluminium is the most prominent candidate to be increasingly used, but welding of aluminium with the conventional electrical resistance spot welding (ERSW) is highly difficult, as the surfaces to be joined must be kept cleaned and free from surface oxides. Moreover, electrode wear limits electrode life to 1000 spots whereas 10,000 spots when welding steel [1]. Friction stir spot welding (FSSW) is an ideal competent process for aluminium welding than ERSW. FSSW is a derivative process of friction stir welding process. FSSW is a single spot joining process, in which a solid-state joining is made between adjacent materials at overlap configuration. This process also eradicates the problems associated with commonly used other single spot joining processes such as mechanical riveting, clinching, and toggle lock [2–5].

There are many publications which studied effects of friction stir spot welding parameters on welding quality. Pan

* Tel.: +98 9369098670; fax: +98 1125233899.
E-mail addresses: reza_teimoori@yahoo.com, reza_teimouri@stu.nit.ac.ir (R. Teimouri).

http://dx.doi.org/10.1016/j.acme.2014.06.005

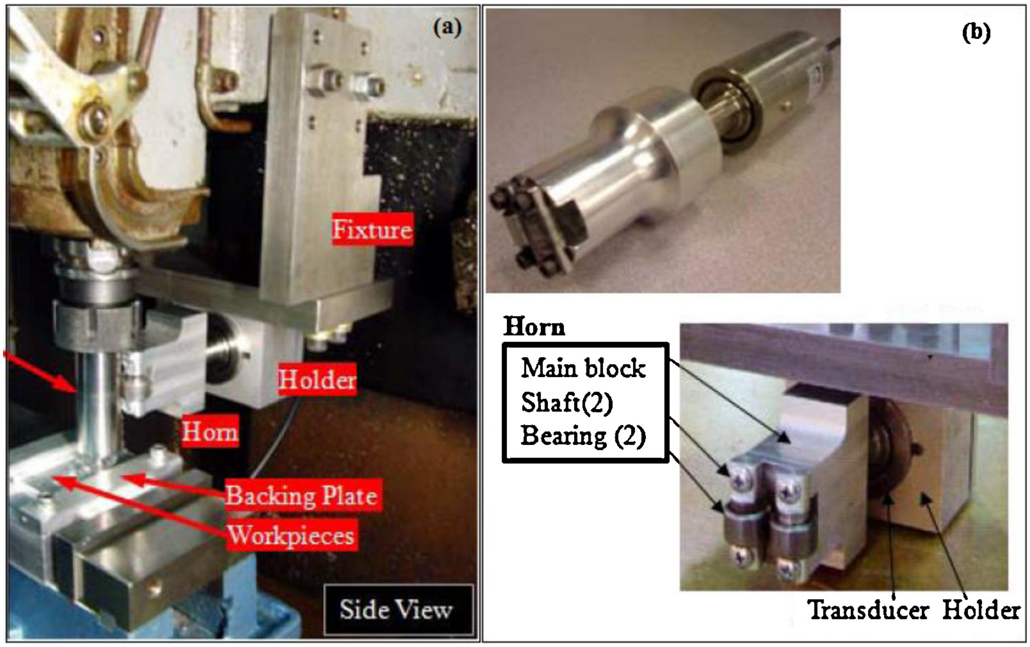

Fig. 1 – (a) Experimental setup. (b) Ultrasonic transducer including rollers.

et al. [6] studied the effect of tool penetration depth at a constant tool rotational speed and reported different failure modes such as interfacial separation at shallow insertion depths, nugget pullout at highest strength, and perimeter failure at deepest insertion. Arul et al. [7] investigated the microstructures and failure mechanisms of FSSW AA5754 aluminium alloy and reported that the failure mechanism was necking and shearing. Mitlin et al. [8] reported that the tool pin of the joints had a lesser effect on the joint shear strength. Karthikeyan and Balasubramanian [9] used response surface methodology and ANOVA to show effect of tool rotary speed, plunge rate, plunger depth and dwell time on lap shear force of AA2024. They showed that plunger rate followed by plunge depth, dwell time and tool rotary speed are the significant factors. Bozkurt and Bilici [10] used Taguchi technique to optimize the FSSW factors to achieve higher lap shear force. They showed that the tool rotary speed is the most predominant factor that affects shear force.

In the past two decades, ultrasonic vibration was successfully assisted with various types of manufacturing process to improve their performance [11–15]. Due to specific properties of US waves, it has positive effect on reducing force and improving heat generation in contact mechanical processes and also ionization and cleaning in non-contact processes. Although, there are numerous works which associated US vibration with manufacturing process, there are not a lot of papers that combined it with friction stir spot welding process. Hence, in the present study applying vibration to improve the weld quality in FSSW of AA6061 can be quite novel.

In the present study, the concepts of ultrasonic welding and friction stir spot welding are integrated to enhance welding performance. Here, Taguchi design of experiments is used to systematically analyze effects of factors on lap shear force and hardness. Also, the analysis of variances is performed to determine contribution of each factor on the performance measures. Then the optimal parameters combination is selected according to combination of Taguchi with grey relational analysis.

2. Experiments

The experiments were conducted on 4301 CNC milling machine with maximum spindle speed of 5000 RPM and power of 15 hp. The vibratory apparatus (model PVSA 1800) made by the Iran Pardis Company was utilized to apply the high frequency vibration on friction stir welding tool. This device includes power supply and transducer which produces frequency of 28 kHz with amplitude of 12 μm. Fig. 1a demonstrates experimental setup including FSSW tool and ultrasonic transducer. To transfer US vibration from ultrasonic horn to FSW tool, a pair of rollers was attached in front of horn. These rollers are in contact with the FSW tool to vibrate it with high frequency. Fig. 1b demonstrates the transducer head including rollers.

To measure the lap shear force, and elongation, the welded specimens have been gripped by grippers of 100 kN servo-controlled universal testing machine and the values of lap-shear force and elongation has been measured.

To monitor the temperature of the welded zone KRYSTAL MY-60 thermocouples was located approximately 12 mm from

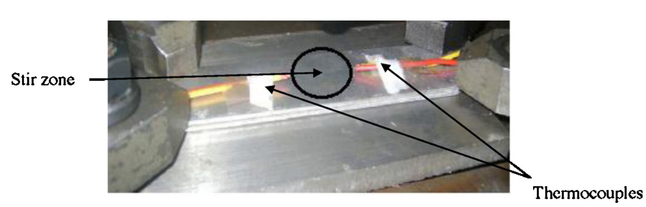

Fig. 2 – Located thermocouples on the sheets.

Table 1 – Chemical compositions of Al 6061 alloy [16].

Components	Mg	Si	Fe	Cu	Cr	Mn	Zn	Ti	Al
Percentage (%)	0.9	0.62	0.33	0.28	0.17	0.06	0.02	0.02	Bal.

the centre of stir zone as shown in Fig. 2. During the process, the temperature rise up drastically and reaches a maximum value and recorded as welding region temperature.

The Vickers hardness upper welded sheets (i.e. the sheet which is in contact with tool shoulder) has been measured by Vickers's micro-hardness testing machine (Make: Shimadzu and Model: HMV-2T) with 0.05 kg load at 15 s.

To welded specimens for metallographic examinations were sectioned to the required sizes from the joint comprising friction stir processed (FSP) zone and then grinded using different grades of emery papers. Final polishing was done using the diamond compound (1 μm particle size) in the disc polishing machine. The polished samples were etched using 10% NaOH to show general flow structure of the alloy. Macro and micro-structural analysis have been carried out using a light optical microscope (VERSAMET-3) incorporated with an image analyzing software (Clemex-Vision). Average grain diameter of the weld region was measured by applying Heyn's line intercept method. The welded specimens were prepared following standard metallographic procedures and the hardness grain diameters were measured at three locations in each specimen. Totally, three measurements were recorded and average of three grain size values is analyzed.

In the present work, the rolled plates of AA6061 with 3 mm thickness were cut into the required sizes (40 mm × 100 mm) by power hacksaw cutting and milling. Then a clamping system was designed to secure the plates in their proper positions. Chemical composition and mechanical properties of AA6061 are presented in Tables 1 and 2 [16], respectively.

A non-consumable tool with cylindrical-conical grooved pin tool made of high carbon steel was used to fabricate the joints. For friction stir spot welding, the tool shoulder and pin profile should be designed specifically for better penetration, heat generation and stirring. This tool was selected due to weld region extension that causes appropriate stirring which improves mechanical properties [17]. Fig. 3 presents the designed tool which was used to conduct experiments.

According to our laboratory experience, it has been decided that ultrasonic vibration, tool rotary speed, tool plunge depth and dwell time are selected as main process factors which have greater influence on welding quality of AA6061. Table 3 presents the process main factors and their working ranges.

Because of extensive range of factors, L_{18} orthogonal array mixed level design ($2^1 \times 3^3$) matrix was selected to minimize the number of experimental observations. Hence, numbers of 18 experimental tests were designed to form design matrix.

Table 2 – Mechanical properties of Al 6061 alloy [16].

Description	Values
Yield strength (MPa)	302
Ultimate tensile strength (MPa)	334
Elongation (%) (A50)	18
Hardness (VHN) (0.05 kg load at 15 s)	125

Table 4 shows the 18 sets of experimental observations along with obtained values of lap shear force and average grain size.

3. Results and discussion

3.1. *Analyzing effects of factors on lap shear force*

In friction stir welding, the configuration of grains and their distribution plays a predominant role on welding quality characteristics. The uniform and finer grain distribution causes increase in weld strength and hardness. On the other hand rough and non-uniform grain distribution leads to poor weld strength, but it improves elongation.

Furthermore, the heat generation is the key factor having great factor on welding performance measures. Increasing heat input causes better material flow and better stirring during process. But when heat input goes beyond a critical value, it may cause some defects on welded region resulting in negative influence on weld quality. The lap shear strength is very sensitive to defect which are formed in welded region. It means that formation of defects like cracks, holes, voids caused by insufficient or excessive heat input can reduce the lap shear strength. According to this explanation, analyzing effect of factors on lap shear force is described as follows.

3.1.1. *US vibration*

Fig. 4 presents effects of process factors along with their contributions which were obtained through ANOVA on lap shear force. From this figure, it is seen that US vibration has positive effect on LSF with highest percentage of contribution (i.e. 38.7%). Images which were obtained from microstructure of welded region showed that applying US vibration leads to

Fig. 3 – Cylindrical-conical grooved pin tool which is used for experiments.

Table 3 – Process factors and their ranges.

Process factors	Unit	Level 1	Level 2	Level 3	Reasons for selection of this range
US vibration	–	Without	With	–	Available range
Tool rotary speed	RPM	800	1200	1600	Lower than 800 RPM speed does not join Al sheets. On the other hand, higher than 1600 RPM speed causes deformation of sheets
Plunge depth	mm	5	5.5	6	At lower than 5 mm depth, the tool does not penetrate in the sheets as well. On the other hand, higher than 6 mm depth leads to deformation of sheets
Dwell time	s	4	6	8	Lower than 4 s dwell time does not join the sheets as well. On the other hand higher than 12 s dwell time causes excessive heat input

Table 4 – Design matrix and obtained values of responses.

No.	Process factors				Reponses	
	US vibration	Tool rotary speed (RPM)	Plunge depth (mm)	Dwell time (s)	Lap shear force (kN)	Hardness (HV)
1	Without	800	5	4	3.21	134
2	Without	800	5.5	6	6.26	109
3	Without	800	6	8	6.08	104
4	With out	1200	5	4	6.06	117
5	Without	1200	5.5	6	9.11	92
6	Without	1200	6	8	8.93	87
7	Without	1600	5	6	6.45	88
8	Without	1600	5.5	8	7.37	69
9	Without	1600	6	4	6.7	81
10	With	800	5	8	8.03	124
11	With	800	5.5	4	8.28	147
12	With	800	6	6	10.40	136
13	With	1200	5	6	11.7	119
14	With	1200	5.5	8	11.8	100
15	With	1200	6	4	11.1	119
16	With	1600	5	8	9.96	96
17	With	1600	5.5	4	9.57	119
18	With	1600	6	6	12.3	108

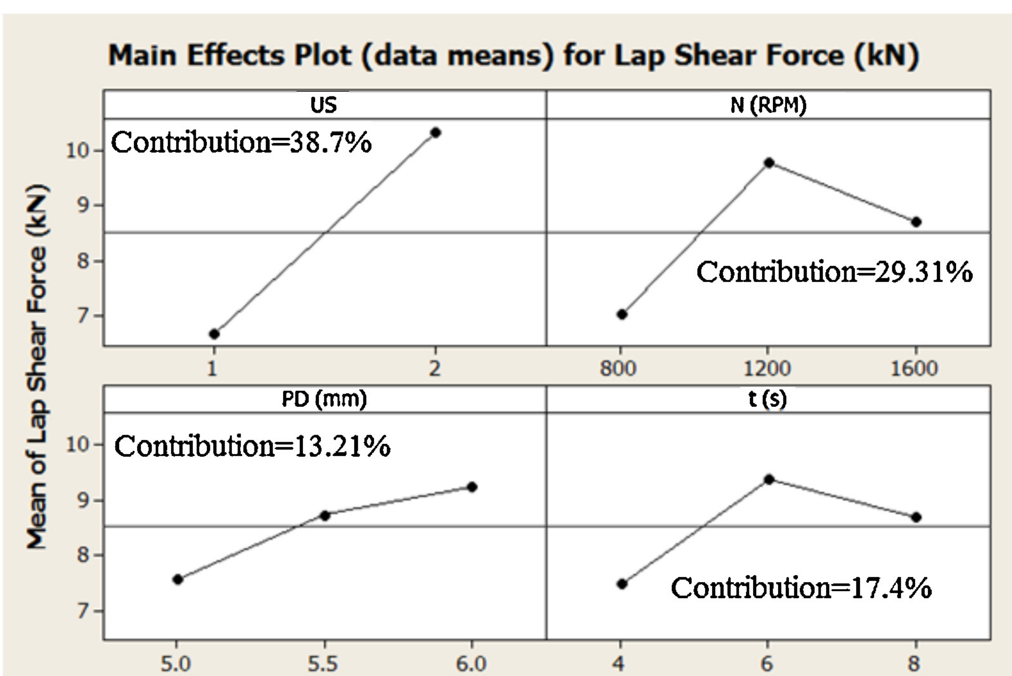

Fig. 4 – Effect of process factors on lap shear force.

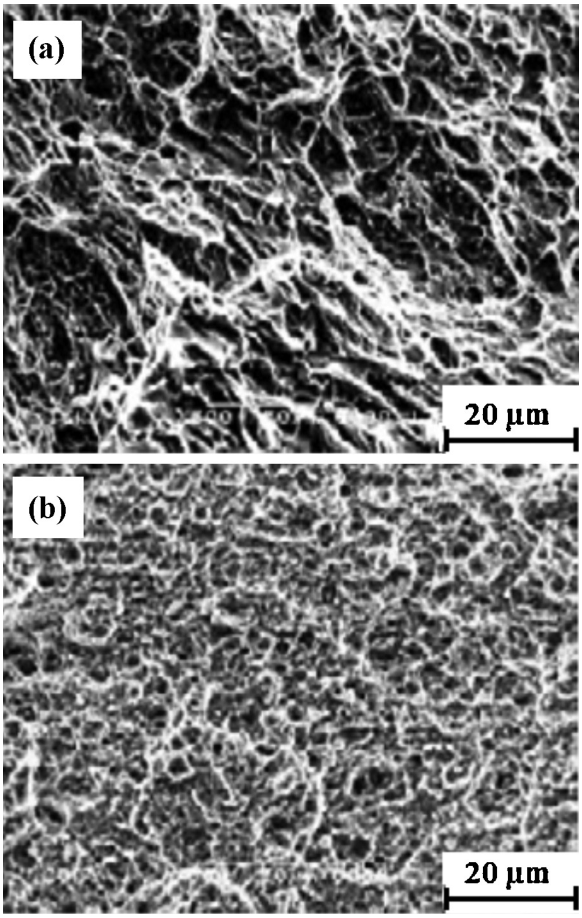

Fig. 5 – SEM micrograph of fracture surface: (a) before applying vibration and (b) after applying vibration.

uniform distribution of grains along the welding direction. Therefore, formation of rougher grains that cause poor shear strength is prevented by applying the vibration. Fig. 5a and b presents SEM photograph of fracture surface before and after applying US vibration. From this figure, it is seen that US vibration causes a finer and uniform grain distribution. The rough type distribution can act as defects and reduces lap shear strength. Therefore, applying vibration leads to high LSF due to uniform and fine grain with higher numbers of grain boundaries.

3.1.2. *Tool rotary speed*

In friction stir spot welding process, tool rotary speed determines strength properties and fracture locations to large extent. The major role of the tool is to generate heat along the welding region. From Fig. 4 it is seen that the lap shear force increases with an increase in tool rotary speed and reaches a maximum value at 1200 RPM. But by further increase in tool rotary speed the LSF decreases correspondingly.

When the tool rotary speed is lower than a critical value (i.e. 1200 RPM in this research), due to insufficient heat generation a poor material mixing is occurred in welding region and it may contain eyelet fracture mode at the top surface of bottom sheet. Fig. 6a presents eyelet fracture mode due to poor material mixing caused by insufficient heat input. On the other hand when the tool rotary speed goes beyond a critical value (i.e. 1200 RPM), due to excessive heat input and high material softening, the flash level between upper and lower sheets increases and prevents appropriate joining of them. Therefore, the LSF decreases. Fig. 6b presents high flash level which is caused by high tool rotary speed. This trend is not just for 1600 RPM; to support the reason, additional experiments were performed and effect of tool rotary speed on 1300 RPM, 1400 RPM and 1500 RPM was investigated. Fig. 7 presents the results. It is seen from the figure that the LSF decreases gradually by increasing in tool rotary speed.

3.1.3. *Plunge depth*

In friction stir spot welding process, by increasing plunge depth of the pin into the sheets, the penetration of tool shoulder also increases and causes higher welding axial force. It causes higher friction and increases the heat generation in the process. Fig. 8 shows that the temperature of the sheets increases by increasing plunging depth under various tool rotary speeds. According to Fig. 4, it is seen that plunging depth has contribution of 13% on lap shear force. By increasing plunging depth the lap shear force also increases. As discussed, increase in plunge depth causes increase in heat input and it yields better material flow and appropriate mixing, therefore the LSF increases. At higher plunge depth the fracture mode is changed from eyelet to partially curved interfacial (Fig. 9) that implies higher force is needed for occurring fracture.

3.1.4. *Dwell time*

In friction stir spot welding the dwell time refers to the contact time between tool shoulder and sheets at given plunge depth. Increase in dwell time causes higher heat generation at welding region. Fig. 10 presents variations of sheet temperature at various dwell times under various tool rotary speeds. From Fig. 4, it is seen that the lap shear force firstly increases by increase in dwell time and reaches a maximum value at 6 s. Then, by further increase in dwell time the lap shear force decreases correspondingly. When the dwell time is lower than a critical value (i.e. 6 s in this research) a poor material mixing occurred due to low heat generation in welding region and causes weak strength properties. On the other hand, when the dwell time goes beyond a critical value, due to excessive heat generation, the grain growth occurred and disturbs uniform distribution of the grains. The rougher grain can act as defects in welded regions and causes a decrease in strength properties. Fig. 11 shows microstructure of grain distribution at various dwell times. From this figure it is seen that by increasing the dwell time the average grain size also increases. From this figure, it is expected that 2 s dwell time causes highest LSF due to its finer grain distribution, but in reality, at a low dwell time material mixing is poor due to insufficient heat input and therefore the LSF is lower consequently. But at high dwell time (i.e. 6 s) the effect rougher grain outperforms material mixing and LSF decreases from its maximum value.

3.2. *Analyzing effects of factors on hardness*

In the friction stir spot welding, hardness of welding region depends on the grain distribution and its average size. According to Hall–Petch law, finer and uniform grain distribution causes

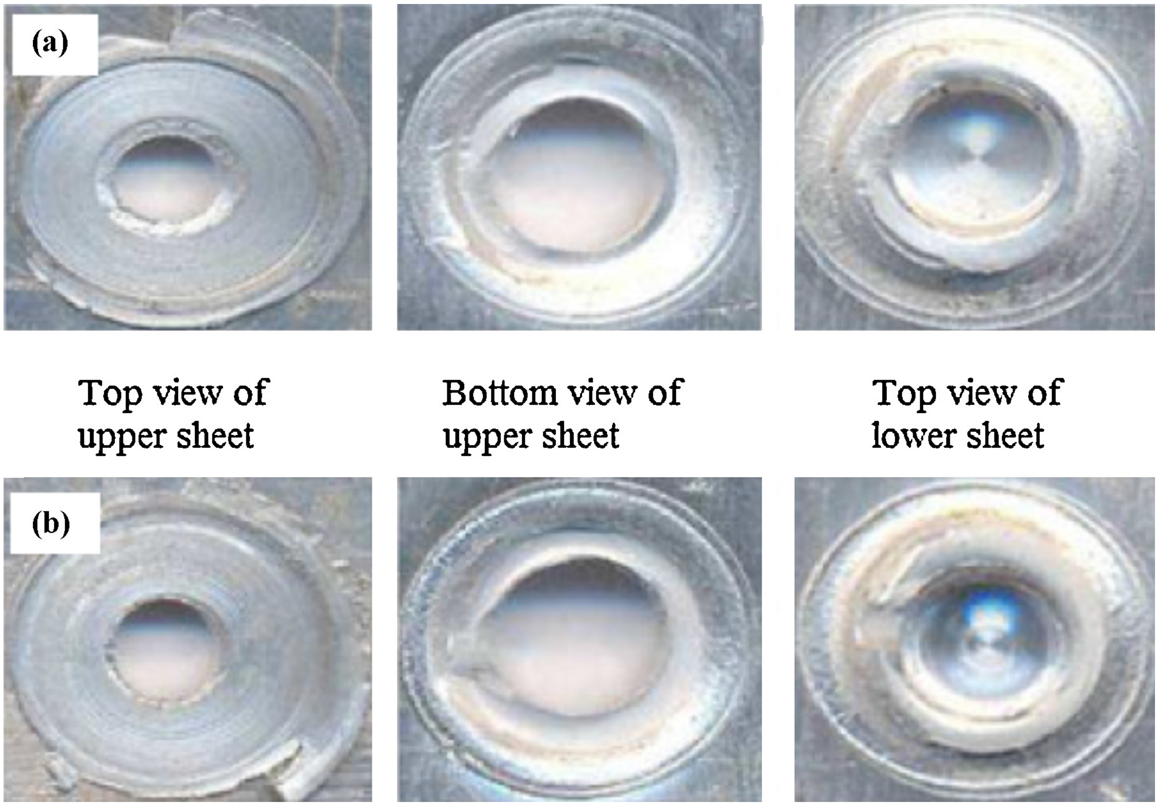

Fig. 6 – Fracture locations for (a) low tool rotary speed strength and (b) high tool rotary speed.

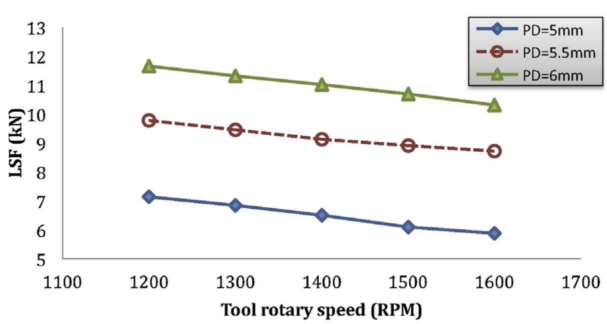

Fig. 7 – Effects of tool rotary speed higher than 1200 RPM on LSF under various plunge depths.

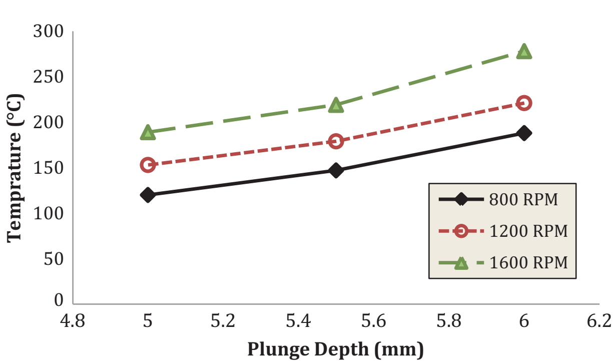

Fig. 8 – Effect of plunge depth on sheet temperature under various tool rotary speeds.

highest hardness in respect with rougher and non-uniform one. Producing heat in welding region causes grain growth and decreases the hardness value. Also producing mechanical vibration in welding region causes fine and uniform distribution and it has positive influence on hardness of FSP region.

Fig. 12 presents effect of process factors along with their contribution percentage on hardness. It is seen from the figure that applying US vibration has positive influence on hardness of welded region. As it is shown in Fig. 13 applying US vibration causes grain refinement and produces a uniform distribution in welded region. A hardness profile which was obtained from welded region showed that applying US vibration increases

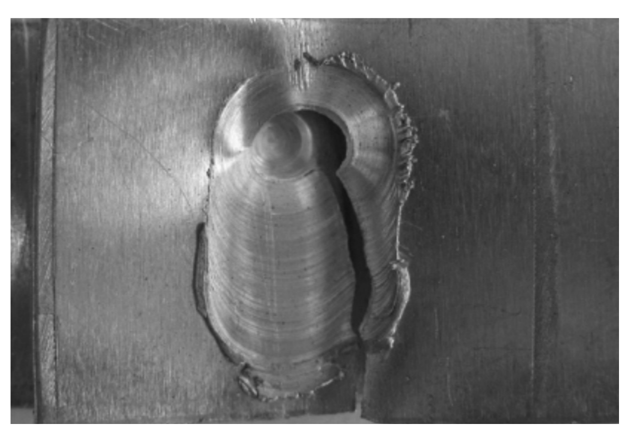

Fig. 9 – Partially curved interfacial fracture mode that is caused by high level of plunging depth.

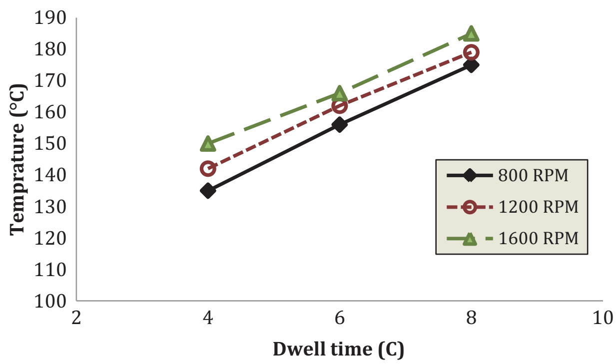

Fig. 10 – Effect of dwell time on sheet temperature under various tool rotary speeds.

hardness not only at stirred zone (SZ), but it enhances the hardness at thermomechanical affected zone (TMAZ) and heat affected zone (HAZ). Fig. 14 presents micro-hardness profile at welding region. The distribution of Vickers hardness was found to be symmetric with respect to the centre of keyhole, showing a W-shaped appearance. The hardness of the welds, which was lower than that of the base metal, reached the minimum hardness of 42.21 HV which was equivalent to 50.7% of the base material hardness. Also, from this figure, it is seen that applying US vibration increases the hardness in all region except base metal.

3.2.1. *Tool rotary speed*

From Fig. 12, it is seen that increase in tool rotary speed causes the hardness values to be reduced. Also, this factor has the greatest impact on hardness. As discussed, the tool rotary speed is the source of heat generation in welding region. Increasing tool rotary speed causes increase in heat input and temperature rise (as shown in Figs. 8 and 10). Therefore, it increases the average grain size and according to the Hall–Petch law, the hardness decreases. Fig. 15 presents hardness profile for various tool rotary speeds. From this figure, it is evident that the hardness decreases by increasing tool rotary speed in SZ, TMAZ and HAZ.

3.2.2. *Plunge depth*

The plunge depth is another factor having influence on hardness. From Fig. 12, it is seen that plunge depth has 10% contribution on hardness. It means that it is the less effective factor among the others. From Fig. 12, it is inferred that by increasing plunging depth the hardness firstly decreases slightly, but by further increase in plunge depth no more reduction observed in hardness value. When the plunge depth increases, the heat input also increases due to higher axial force and higher friction between tool shoulder and the sheet. Hence the grain size increases and hardness decreases according to Hall–Petch law. By further increase in plunge depth it is expected that the hardness decreases more due to grain growth, but the mechanical working also increases at high level of plunge depth and prevents more grain growth. For this reason the hardness value remains constant.

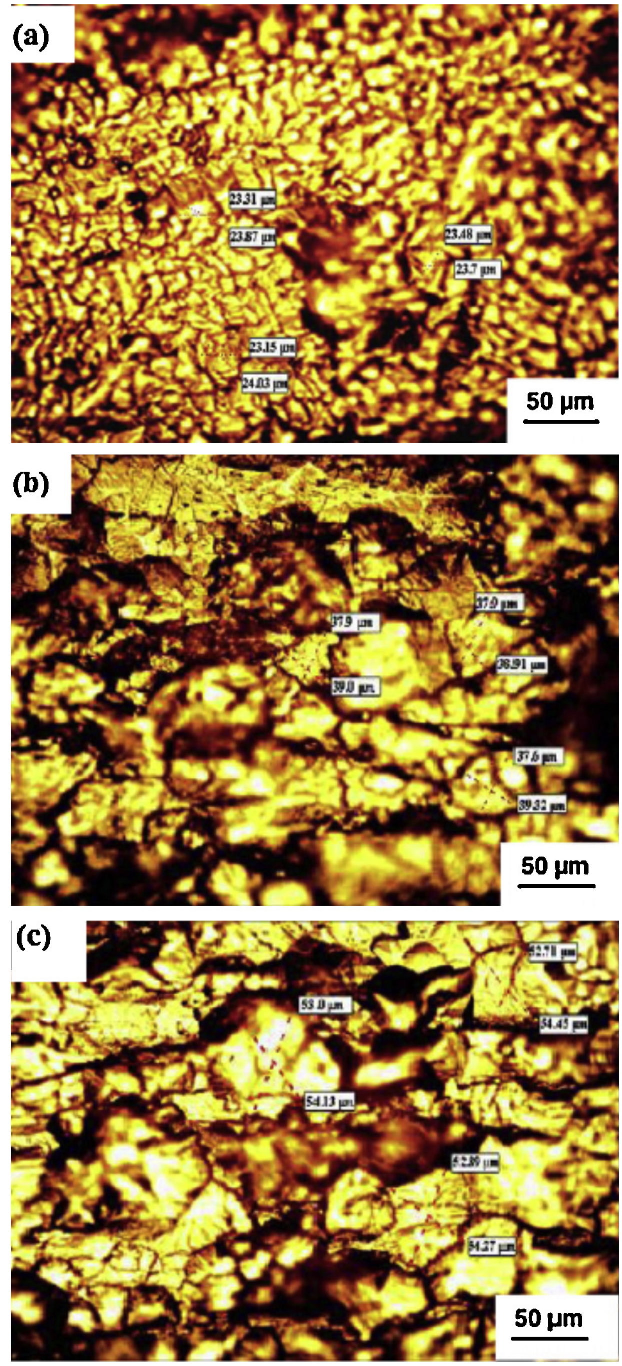

Fig. 11 – Grain distribution at various dwell times: (a) 2 s (D_{ave} = 23.6 μm), (b) 4 s (D_{ave} = 38.15 μm) and (c) 6 s (D_{ave} = 53.21 μm).

3.2.3. *Dwell time*

The effect of dwell time is similar to tool rotary speed, completely. According to Fig. 12, it is visible that increase in dwell time causes hardness values to be increased. As discussed, by increasing dwell time the heat input also increases and causes grain growth in welding region. Therefore, based on Hall–Petch law the hardness of stirred zone along with thermomechanical affected zone and heat

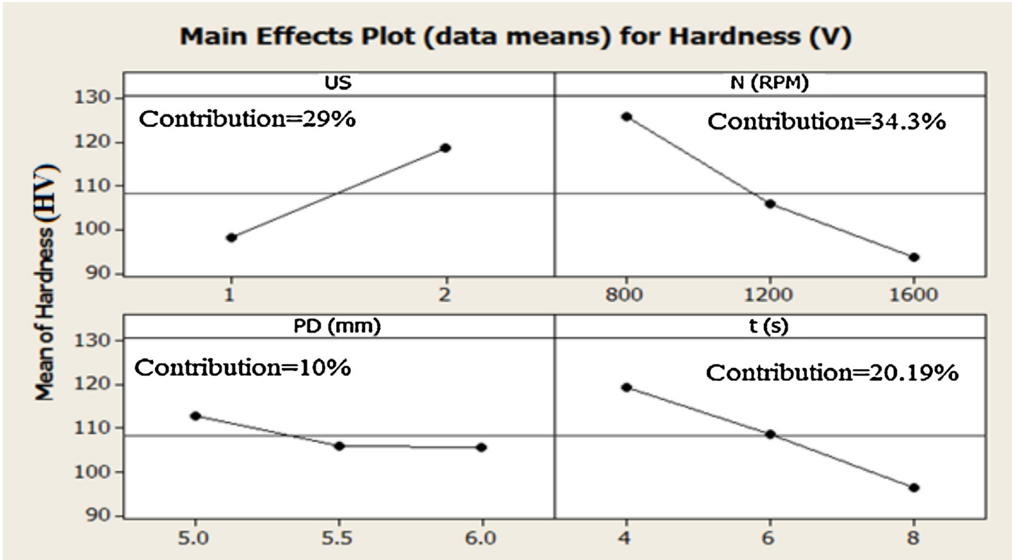

Fig. 12 – Effect of process factors on hardness.

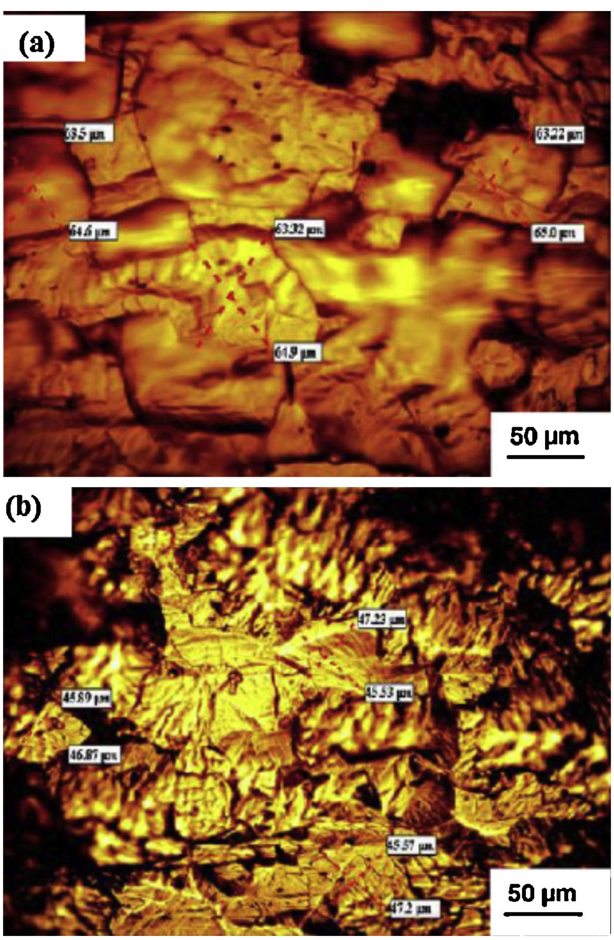

Fig. 13 – Microstructure of welded region (a) before applying US vibration (D_{ave} = 64.41 μm) and (b) after applying US vibration (D_{ave} = 43.3 μm).

affected zone decrease correspondingly. The hardness profile for various dwell times is visible in Fig. 16.

4. Optimization

In the present study the grey relational analysis was used to find optimal solutions which cause achievement of maximum lap shear force and hardness. The step by step implementation of grey relational analysis along with details and equations are found in Ref. [18]. Various stages for implementation are:

- Normalization
- Calculation of original sequence
- Calculation of grey relational coefficient
- Calculation of grey relational grade
- Response of factors to grey relational grade
- Confirmation

Table 5 presents normalized values of responses, original sequence (Δ_{0i}), grey relational coefficient and grey relational grades for lap shear force and hardness. In this work the weight factors of 0.5 is considered for both lap shear force and hardness. By applying this method the multi-criteria optimization problem has been transformed into a single equivalent objective function optimization problem using the combination of Taguchi approach and grey relational analyses. Higher value of grey relational grade corresponds factor combination which is said close to optimal. The mean response results for the overall grey relational grade is shown graphically in Fig. 17.

4.1.1. *Selection of optimal combination*

From this figure it is seen that applying US vibration and selections of 1200 RPM tool rotary speed, 6 mm plunge depth and 6 s dwell time causes highest value of grey relational grade

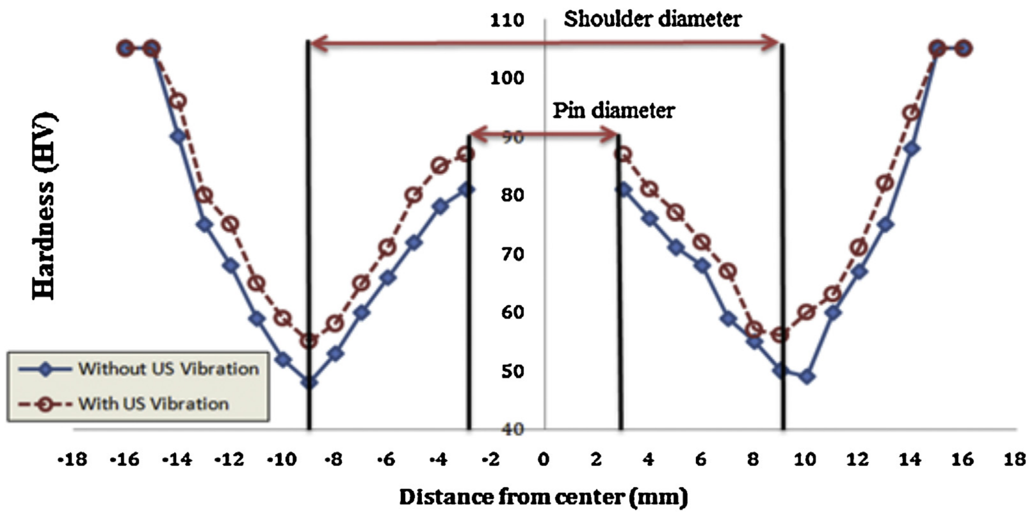

Fig. 14 – The hardness profile of welded region showing effect of US vibration.

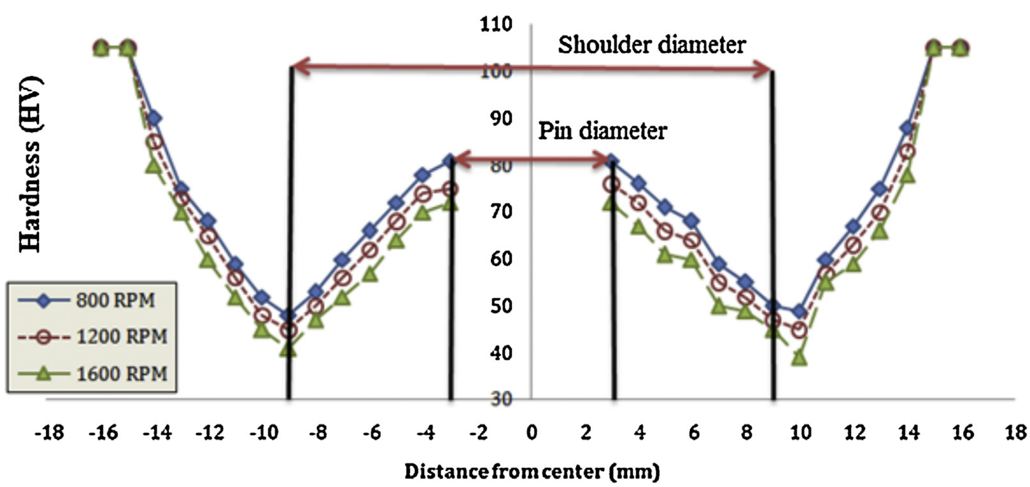

Fig. 15 – The hardness profile of welded region showing effect of tool rotary speed.

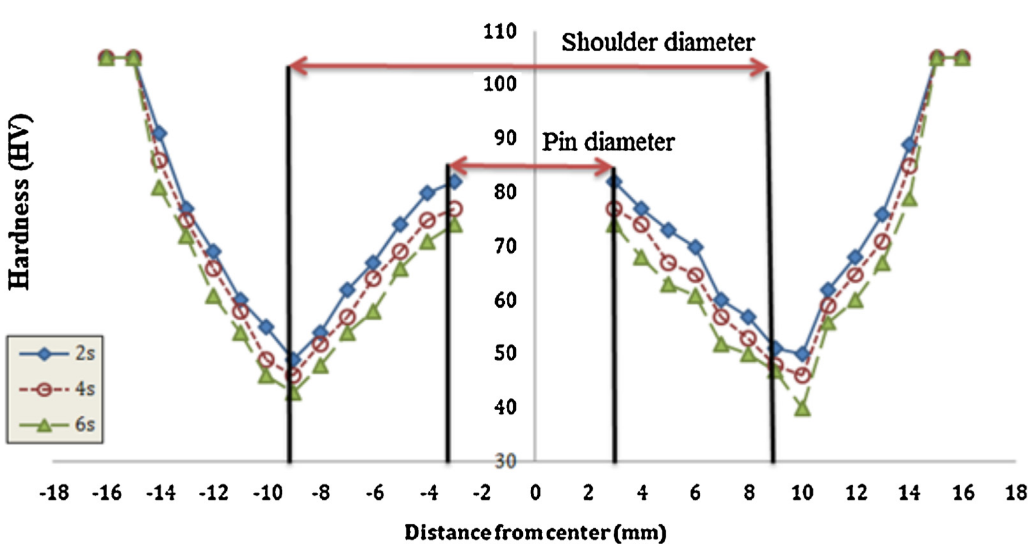

Fig. 16 – The hardness profile of welded region showing effect of dwell time.

Table 5 – Grey relational generations, Δ_{0i}s, grey relational coefficients, and grey relational grades of experimental data.

No.	Grey relational generation		Δ_{0i}		Grey relational coefficient		Grey relational grade	
	LSF	H	LSF	H	LSF	H	Value	Rank
1	0	0.8338	1	0.1667	0.3333	0.75	0.2708	10
2	0.3355	0.5128	0.6645	0.4872	0.4294	0.5056	0.234	14
3	0.3157	0.4487	0.6843	0.5513	0.4222	0.4756	0.2245	15
4	0.3135	0.6154	0.6865	0.3846	0.4214	0.5652	0.2467	12
5	0.6491	0.2949	0.3509	0.7051	0.5876	0.4149	0.2506	11
6	0.6293	0.2308	0.3707	0.7692	0.5743	0.3939	0.242	13
7	0.3564	0.2436	0.6436	0.7564	0.4372	0.398	0.2088	16
8	0.4576	0	0.5424	1	0.4797	0.3333	0.2032	18
9	0.3839	0.1538	0.6161	0.8462	0.448	0.3714	0.2049	17
10	0.5303	0.7051	0.4697	0.2949	0.5156	0.629	0.2862	8
11	0.5578	1	0.4422	0	0.5307	1	0.3827	1
12	0.791	0.859	0.209	0.141	0.7052	0.78	0.3713	3
13	0.934	0.641	0.066	0.359	0.8834	0.5821	0.3664	4
14	0.945	0.3974	0.055	0.6026	0.9009	0.4535	0.3386	6
15	0.968	0.641	0.132	0.359	0.7911	0.5821	0.3433	5
16	0.7426	0.3462	0.2574	0.6538	0.6602	0.4334	0.2734	9
17	0.6997	0.641	0.3003	0.359	0.6248	0.5821	0.3017	7
18	1	0.5	0	0.5	1	0.5	0.375	2

and guarantee maximum lap shear force as well as maximum hardness. Therefore, the combination of $US_2N_2d_3t_2$ is optimum.

4.1.2. *Discussion about the optimal results*

Applying vibration improves both lap shear force and hardness therefore applying vibration is desirable. About tool rotary speed it can be said that 1200 RPM causes the highest value of LSF and middle value of hardness. But in multi-objective optimization regarding weight factor of 0.5, it is logical that the 1200 RPM speed has highest response to grey relational grade. About the dwell time the same scenario exists. It means that 6 s dwell time causes highest LSF, on the other hand, 4 s dwell time leads to maximum hardness. But, due to equal weight factors for the responses, the 6 s dwell time has the greatest response to grey relational grade. Furthermore, selection of the highest value of plunge depth, i.e. 6 mm causes highest lap shear force. On the other hand there is no difference between the hardness value in 5.5 and 6 mm plunge depth. Thus, selection of 6 mm plunge depth causes highest response to grey relational grade.

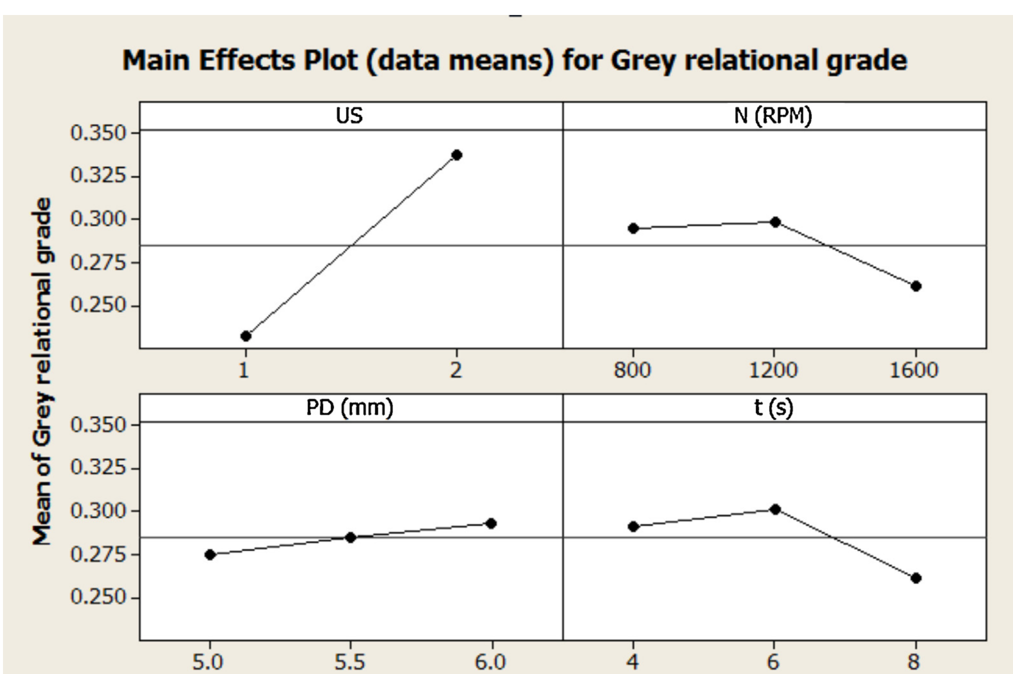

Fig. 17 – Response of process factors to grey relational grade.

Table 6 – Results of confirmatory experiment.

	Initial US-FSSW parameters	Optimal US-FSSW parameters	
		Experiment	Prediction
Setting level	$US_1N_1d_1t_1$	$US_2N_2d_3t_2$	$US_2N_2d_3t_2$
Lap shear force	3.21	9.12	–
Hardness	134	139	–
Means of grey relational grade	0.2708	0.4087	0.4019

Improvement of grey relational grade from first setting level to optimal setting level = 33.59%.

4.1.3. *Confirmation through experiment*

After evaluating the optimal parameter settings, the next step is to predict and verify the enhancement of quality characteristics using the optimal parametric combination. For this reason, a confirmatory experiment is conducted with the obtained optimum factor and the values of LSF, hardness and grey relational grade are calculated. If the value of grey relational grade which is obtained through confirmatory experiment is near to value which is obtained through estimation, the proposed methodology will be efficient in solving this optimization problem. Table 6 represents the comparison of the estimated grey relational grade with that of actual obtained through experiments at optimum factor combination. It is seen that good agreement between the two has been observed. This proves the utility of the proposed approach in relation to product/process optimization, where more than one objective has to be fulfilled simultaneously.

5. Conclusion

In the present work, a new hybrid welding process namely ultrasonic assisted friction stir spot welding has been introduced and characterized. Here effects of US vibration along with tool rotary speed, plunge depth and dwell time on lap shear force and hardness have been studied. Then the grey relational analysis was used to find optimal combination of factors that causes maximum lap shear force and hardness simultaneously. The obtained results are summarized as follows:

- Association of ultrasonic vibration with friction stir spot welding improves lap shear force and hardness.
- The operational range of process parameters for high lap shear force were achieved by selection vibratory tool, 1200 RPM rotary speed, 6 mm plunge depth and 6 s dwell time.
- The operational range of parameters for achieving high hardness were achieved by selection vibratory tool, 800 RPM rotary speed, 5 mm plunge depth and 4 s dwell time.
- Optimization through grey relational analysis showed that applying US vibration and selections of 1200 RPM tool rotary speed, 6 mm plunge depth and 6 s dwell time causes the highest value of grey relational grade and guarantee maximum lap shear force as well as maximum hardness.

Appendix A. Abbreviations

FSW friction stir welding
FSSW friction stir spot welding
ERSW electrical resistance welding
FSP friction stir processes
USW ultrasonic welding
US ultrasonic vibration
AA aluminium alloy
N tool rotary speed
PD plunge depth
t dwell time
LSF lap shear force
HV hardness Vickers

REFERENCES

[1] F.G. Armao, R.S. Long, Joining techniques for aluminum castings, extrusions and sheet, in: Winter EFM Conf., 1992.
[2] T. Iwashita, Method and apparatus for joining, US Patent 6,601,751 B2, 2003.
[3] R. Sakano, K. Murakami, K. Yamashita, T. Hyoe, M. Fujimoto, M. Inuzuka, U. Nagao, H. Kashiki, Development of spot FSW robot system for automobile body members, in: Proceedings of the Third International Symposium of Friction Stir Welding, Kobe, Japan, 27–28 September, 2001.
[4] S. Sakaguchi, Resistant spot welding of aluminum alloy, Journal of Light Metal Welding and Construction 17 (3) (1979) 126–134 (in Japanese).
[5] D. Wang, S. Liu, Z. Cao, Study of friction stir welding of aluminum, Journal of Materials Science 39 (2004) 1689–1693.
[6] T.Y. Pan, A. Joaquin, D.E. Wilkosz, L. Reatherford, J.M. Nicholson, Z. Feng, M.L. Santella, Spot friction welding for sheet aluminum joining, in: 5th International Symposium on Friction Stir Welding, The Welding Institute, Metz, France, 2004, paper no. 11A-1.
[7] S.G. Arul, T. Pan, P.C. Lin, J. Pan, Z. Feng, M.L. Santella, Friction Spot Joining of an Extruded Al–Mg–Si Alloy, SAE International, Warrendale, PA, 2005.
[8] D. Mitlin, V. Radmilovic, T. Pan, J. Chen, Z. Feng, M.L. Santella, Structure properties relations in spot friction welded (also known as friction stir spot welded) 6111 aluminum, Materials Science and Engineering A 441 (2006) 79–96.
[9] R. Karthikeyan, V. Balasubramanian, Predictions of the optimized friction stir spot welding process parameters for joining AA2024 aluminum alloy using RSM, International Journal of Advanced Manufacturing Technology 51 (2010) 173–183.
[10] Y. Bozkurt, M.K. Bilici, Application of Taguchi approach to optimize FSSW parameters on joint properties of dissimilar AA2024-T3 and AA5754-H22 aluminum alloys, Materials and Design 51 (2013) 513–521.
[11] R. Teimouri, H. Baseri, Experimental study of rotary magnetic field-assisted dry EDM with ultrasonic vibration of workpiece, International Journal of Advanced Manufacturing Technology 67 (2013) 1371–1384.
[12] S. Skoczypiec, Research on ultrasonically assisted electrochemical machining process, International Journal of Advanced Manufacturing Technology 52 (2011) 565–574.
[13] V.L. Babitsky, A.N. Kalashnikov, A. Meadows, A.A.H.P. Wijesundara, Ultrasonically assisted turning of aviation materials, Journal of Materials Processing Technology 23 (1–3) (2003) 157–167.

[14] K. Marcel, Z. Marek, P. Jozef, Investigation of ultrasonic assisted milling of aluminum alloy AlMg4.5Mn, Procedia Engineering 69 (2014) 1048–1053.
[15] H.C. Mult, G. Spur, S.E. Holl, Ultrasonic assisted creep feed grinding of ceramics, Journal of Materials Processing Technology 62 (4) (1996) 287–293.
[16] K. Elangovan, V. Balasubramanian, S. Babu, Predicting tensile strength of friction stir welded AA6061 aluminum alloy joints by a mathematical model, Materials and Design 30 (2009) 188–193.
[17] G. Buffa, G. Campanile, L. Fratini, A. Prisco, Friction stir welding of lap joints: influence of process parameters on the metallurgical and mechanical properties, Journal of Materials Science and Engineering A 519 (2009) 19–26.
[18] R. Bagherian-Azhiri, R. Teimouri, M. Ghasemi-Baboly, Z. Leseman, Application of Taguchi, ANFIS and grey relational analysis for studying, modeling and optimization of wire EDM process while using gaseous media, International Journal of Advanced Manufacturing Technology 71 (2014) 279–295.